PCCP

Dynamic Article Links

Cite this: *Phys. Chem. Chem. Phys.*, 2011, **13**, 4842–4845

www.rsc.org/pccp

COMMUNICATION

Insights into scanning probe high-field chemistry of diphenylgermane†

Stephanie E. Vasko,[ab] Wenjun Jiang,[c] Renyu Chen,[d] Robert Hanlen,[a] Jessica D. Torrey,[a] Scott T. Dunham*[acd] and Marco Rolandi*[a]

Received 13th October 2010, Accepted 19th January 2011
DOI: 10.1039/c0cp02150d

Experiments and simulations are used to elucidate a new class of chemical reactions occurring near the tip–sample interface during high field chemistry of diphenylgermane. Current data during writing and bias dependent growth rate are analyzed, supplemented with data from ionization mass spectrometry, and compared with the simulation results.

Scanning probe microscopes can confine chemical reactions at the nanoscale through the delivery of specific stimuli[1] or reactants[2] to a small area of the sample surface. This confinement can be used to produce chemical patterns with well defined functionality by exploiting macroscale reactions such as "click" chemistry and Diels–Alder coupling.[3,4] Nanoscale thermochemistry is also available with heated tips to create 2D and 3D patterns in reduced graphene,[5] or polymeric[6,7] and macromolecular resists.[8] Another common strategy for reaction confinement is to apply a moderate bias between the tip and the sample. In a humid environment, the water meniscus at the tip–sample interface is often described as a nanoscale electrochemical cell where H^+ and OH^- are created. The extremely high electric field ($>10^9$ V m^{-1}) arising from tip–sample proximity directs the desired ions onto the sample, which is oxidized or reduced depending on bias. In this fashion, the field-induced oxidation or reduction of conducting substrates[9–11] and organic monolayers[12,13] has been demonstrated. Recent efforts at replacing the water meniscus in the tip–sample gap with menisci of organic and inorganic molecules have introduced a novel class of chemical reactions that do not seem to follow a clear electrochemical pathway. It has been previously theorized that these reactions are triggered by the high electric field and are analogous to the processes occurring in field ionization microscopes.[14] These reactions include self-assembled monolayer activation,[15–17] polymer cross linking,[18] sulfur polymerization,[19] and localized synthesis of carbon nanostructures from liquid[20–23] or gaseous precursors.[24] Kinetic studies of carbon growth have found trends in agreement with the high-field conjecture, but a conclusive model for the localized high-field chemistry is still lacking. Most recently, the localized high-field reaction of diphenylgermane *via* AFM has demonstrated the direct-write of germanium nanofeatures.[25] Remarkably, this process produces carbon-free germanium, suggesting that, unlike the growth process of carbon nanostructures, the reaction of the inorganic precursor follows a very specific pathway. Diphenylgermane thus presents a model system to better understand the high-field chemistry occurring near the tip–sample interface.

In this communication, we attempt to elucidate the fundamental processes occurring in the high-field reaction of diphenylgermane (DPG) by comparing experimental results from AFM writing and electron ionization mass spectroscopy with simulations. In brief, a biased AFM tip traces desired shapes along the silicon sample while a diphenylgermane meniscus is condensed *via* saturated vapor at the tip–sample interface (Fig. 1a). Due to tip–sample proximity, even a moderate 10 V bias induces an electric field with peak values above 10^9 V m^{-1} (Fig. 1b) near the tip–sample interface. Here, we propose that the high electric field leads to electrons tunneling from the AFM tip to the DPG molecule creating a temporary negative ion (TNI).[26] In the high electric field, the charged DPG then fragments, leading to carbon-free germanium nanostructures. We propose a reaction where phenyl groups and hydrogens leave the diphenylgermane as benzene, which is a stable leaving group. The benzene most likely dissolves into the DPG meniscus. The germanium, in the form of ions or radicals, then condenses onto the surface to form nanostructures (Fig. 1a). Carbon-free low-temperature synthesis of germanium nanowires from DPG has previously been demonstrated,[27] suggesting that DPG is a viable precursor for this chemistry.

To test the first part of our model, we have measured the current across the tip–sample interface with a stationary tip as a function of applied voltage and compared it with the prediction of simulations that consider non-local tunneling across the SiO_2 layers on the substrate and tip (Fig. 2). During this measurement, the use of the DPG meniscus ensures that all the current measured goes through the reaction area. The onset of the current at 8 ± 1 V corresponds to the predicted onset for electron emission from the AFM tip into the diphenylgermane liquid. For negative voltages as low as −20 V (sample),

[a] *Department of Materials Science & Engineering, University of Washington, 302 Roberts Hall Box 352120, Seattle, WA, USA. E-mail: rolandi@u.washington.edu; Fax: 206 543 3100; Tel: 206 221 0309*
[b] *Department of Chemistry, University of Washington, Seattle, WA, USA*
[c] *Department of Physics, University of Washington, Seattle, WA, USA*
[d] *Department of Electrical Engineering, University of Washington, Seattle, WA, USA. E-mail: dunham@u.washington.edu*
† Electronic supplementary information (ESI) available: Experimental and simulation details. See DOI: 10.1039/c0cp02150d

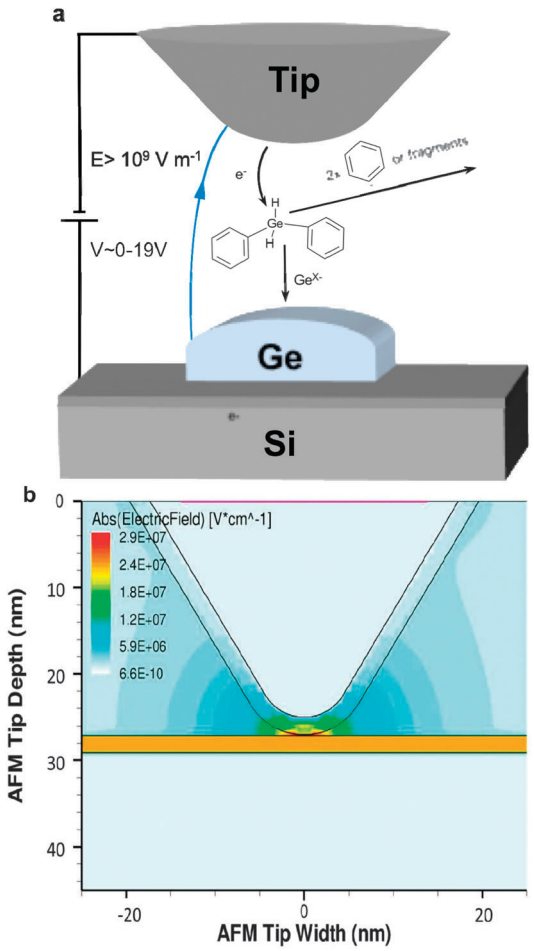

Fig. 1 (a) Schematic of the probe-sample geometry and the proposed chemical reaction of DPG for Ge nanostructure AFM direct-write. (b) Calculation of electric field distribution (V cm^{-1}) for a Si AFM tip in diphenylgermane in contact with Si substrate (3.5 nm oxide) biased at 10 V. The calculation includes distribution of ionized precursors in DPG and thin oxide on both tip and substrate.

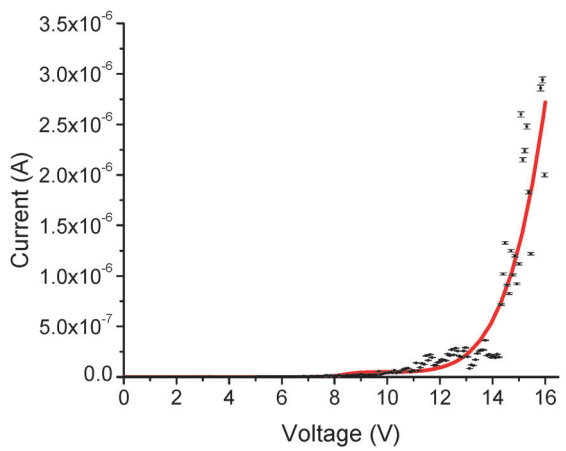

Fig. 2 Current *versus* applied voltage (measured positive on the sample) obtained in a single *I–V* sweep with a stationary tip (black points). Simulation of current between sample and tip including non-local tunneling model using a structure matched to experimental conditions (red line).

the current follows linear behavior and no deposition occurs. For positive voltages on the sample, a reaction threshold is observed after the onset of field emission. These results are consistent with previous STM observations of field emission and dielectric breakdown in liquid octane.[28]

Insights into the potential fragmentation routes were provided by density functional theory (Table 1). From these calculations, it emerges that electron capture by DPG greatly reduces the dissociation energy, with the lowest energy occurring for the separation of a benzene molecule from DPG. This dissociation route becomes energetically favorable upon electron capture. These calculations are consistent with our proposed model. Ideally, one would directly verify the reaction pathway by collecting intermediate fragments during AFM writing. However, the sub-attomolar quantities of precursor reacted in this process do not allow for such analyses. To overcome these issues, mass spectrometry data from electron ionization was collected (Fig. 3). A similar strategy was previously adopted to explain STM induced reactions of gaseous precursors.[26] In such an experimental set-up, a field equivalent to the one present during AFM writing cannot be induced. However, using mass spectrometry of the precursor liquid, electron attachment fragmentation routes can still be verified. In an effort to reproduce the AFM conditions, the lowest energy electrons (17 eV) that would give a reasonable signal to noise ratio were employed. This energy is comparable to the energy of the electrons emitted from the AFM tip. From this data, it is clear that during electron ionization the route that leads to a diphenylgermane fragmenting into benzene and a phenylgermane radical is a favorable one. The signature for fragments of Ge attached to other smaller organic fragments does not appear in this low-energy electron spectrum in agreement with the AFM findings of creating a carbon-free Ge product.

To further understand the writing process, we have produced features with different bias voltages. To minimize the effects of the growth material accumulating under the tip, we translate the tip at a constant rate (1 μm s^{-1}) while writing germanium lines on the sample. The onset voltage for writing occurs at 8 ± 2 V and typically corresponds with the onset of the field emission current, but varies more widely than the latter. We attribute the somewhat large variability of the writing onset to the disparity in tip radius of curvature and tip shape. SEM investigation before and after writing suggests that the tip changes shape continuously during writing, thus affecting its field emission properties. It is interesting to note that high-quality patterns with relatively small line edge roughness can be produced by a somewhat blunt and irregular tip. After onset, the germanium lines grow wider and taller

Table 1 Dissociation energies (E_d) for diphenylgermane as a function of system charge and identity of the removed fragment

	System charge (q)		
Fragment	0	−1	−2
$(C_6H_5)^0$	3.77	1.84	1.83
$(C_6H_5)^-$	7.25	2.71	0.91
$(C_6H_6)^0$	1.05	−0.10	−0.08

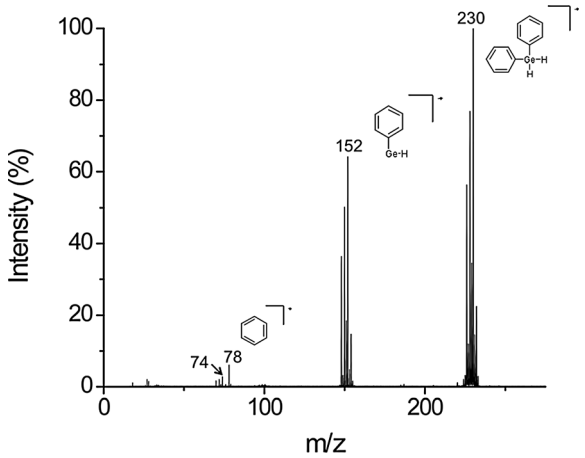

Fig. 3 Electron Ionization Mass spectroscopy data acquired from liquid diphenylgermane using 17 eV ionization electrons. The signature of positive molecular fragments corresponding to the diphenylgermane molecular ion (230 amu), phenylgermane radical cation (152 amu), benzene cation (78 amu), and germanium radical cation (74 amu) are clearly discernible and dominate the spectra. The spectra are consistent with the isotopic abundances of C and Ge as well as loss of 1 additional H from the Ge complexes.

with increasing voltage up to *ca.* 20 V positive on the sample. Above 20 V, the deposition becomes erratic and microscopic irregular features are often observed. These appear to be caused by small explosive discharges occurring near the tip–sample interface.[18] Typical results from the deposition are shown in Fig. 4. To minimize tip convolution effects, the images were recorded in air in tapping mode with a new tip ($r < 10$ nm).

For regular deposition, the line width starts at 40 nm (8 V) and reaches a maximum width of *ca.* 80 nm (19 V). The feature height follows a similar trend starting at 0.5 nm for deposition occurring at 8 V and reaching its maximum of 3.5 nm for deposition occurring at 19 V. The height increases sevenfold from the minimum to the maximum voltage, while the width only increases twofold. This anisotropic growth trend may be caused by the direction and gradient of the electric field that likely directs the deposition of the reactive species. Another factor to be considered is that the maximum width of the DPG meniscus likely laterally confines the reaction.[29]

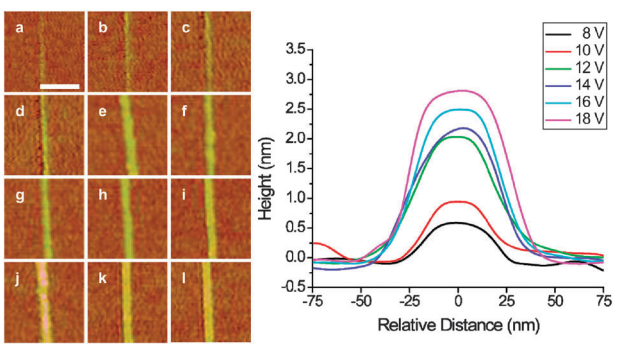

Fig. 4 Left: Tapping mode AFM images of germanium nanostructures written at 8–19 V respectively at 1 μm s^{-1}. Scale bar is 250 nm. Height scale from dark brown to light yellow is 10 nm. Right: Cross-sections of the germanium features. For clarity, only the plots at even voltages are shown.

To estimate the reaction rate, we measure the average volume of germanium deposited per second as a function of voltage (Fig. 5a). With increased voltage, more material is deposited per unit time. This trend has also been observed for high-field deposition of carbon from CO_2.[24] However, the volume of material deposited does not increase as fast as the field emitted current that is measured during writing (ESI†). To further investigate this phenomenon, we calculate the inverse of the number of electrons required to react a DPG molecule and yield a germanium atom (Fig. 5b). This value is an estimate of the reaction efficiency as a function of average electron energy.

This is an estimate of the reaction efficiency as a function of average electron energy. From these data it is clear that most electrons cross the tip–sample interface without leading to the dissociation and deposition of a DPG molecule. This is a confirmation that the reaction occurring at the tip–sample interface is not purely electrochemical in nature, where one would expect a one-to-one correlation of electrons to reacted molecules. A significantly less efficient electron attachment process is involved in this reaction. At higher voltage bias (higher electron energy), reaction efficiency is decreased. This attachment process was already observed in the formation of TNIs during the reaction of silane precursors using STM. However, in the STM work,[26] where the tip is further away from the surface, the electric field is too small[14] to be responsible for direct field-induced dissociation of the silane. In this work, the electric field

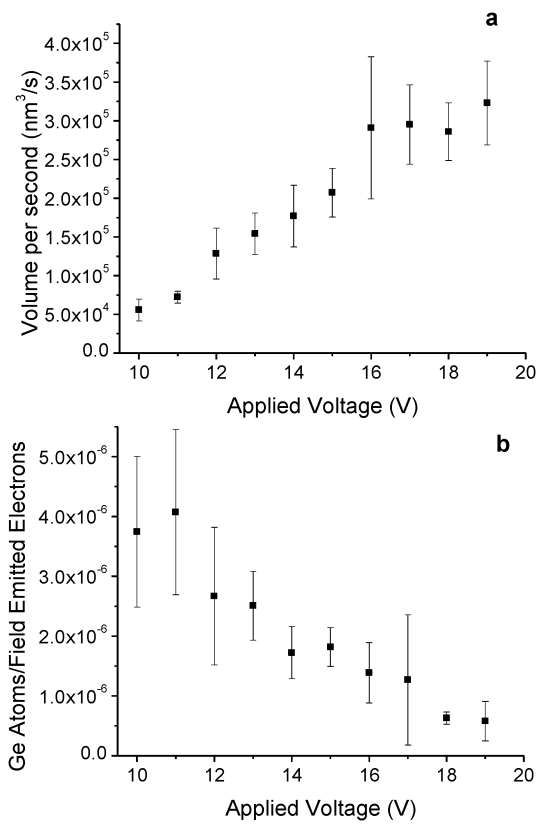

Fig. 5 (a) Germanium volume write rate as a function of tip–sample bias. (b) Plot of the number of germanium atoms deposited per field emitted electron (reaction efficiency) as a function of voltage. Data for voltages lower than 10 V, where not all series resulted in deposited germanium, are omitted for clarity.

is above the reaction threshold[26] and likely plays a role in the dissociation of the TNIs to yield the desired product.

In conclusion, we have experimentally investigated and modeled *via* simulations the mechanisms of Ge nanostructure growth by the high-field reaction of diphenylgermane. We propose a model that involves electron field emission from the tip, followed by electron attachment with formation of temporary negative ions and high field fragmentation. We thus confirm that the reaction of the diphenylgermane precursor at the tip–sample interface is neither purely electrochemical in nature nor purely high-field activated and follows the same trends as the previously reported carbon deposition from organic precursors. This work contributes to the understanding of the possible reactions occurring at the tip–sample interface and can be used to expand the scope of this technique. Examples include using different organometallic precursors for the direct-write of a broad variety of materials.

Acknowledgements

Funding from the National Science Foundation under CHE-1012419, the University of Washington Center for Nanotechnology (S.E.V.) NSF-IGERT (#DGE-050457), a 3M Untenured Faculty Grant, Intel, and the University of Washington are kindly acknowledged. We are grateful to Dr Martin Sadilek of the UW Chemistry Mass Spectrometry facility for assistance with some of the experiments and insightful discussions.

References

1 R. Garcia, R. V. Martinez and J. Martinez, *Chem. Soc. Rev.*, 2006, **35**, 29–38.
2 D. S. Ginger, H. Zhang and C. A. Mirkin, *Angew. Chem., Int. Ed.*, 2004, **43**, 30–45.
3 B. Gotsman, U. Duerig, J. Frommer and C. J. Hawker, *Adv. Funct. Mater.*, 2006, **16**, 1499–1505.
4 D. A. Long, K. Unal, R. C. Pratt, M. Malkoch and J. Frommer, *Adv. Mater.*, 2007, **19**, 4471–4473.
5 Z. Wei, D. Wang, S. Kim, S.-Y. Kim, Y. Hu, M. K. Yakes, A. R. Laracuente, Z. Dai, S. R. Marder, C. Berger, W. P. King, W. A. de Heer, P. E. Sheehan and E. Riedo, *Science*, 2010, **328**, 1373–1376.
6 O. Fenwick, L. Bozec, D. Credgington, A. Hammiche, G. M. Lazzerini, Y. R. Silberberg and F. Cacialli, *Nat. Nanotechnol.*, 2009, **4**, 664–668.
7 A. W. Knoll, D. Pires, O. Coulembier, P. Dubois, J. L. Hedrick, J. Frommer and U. Duerig, *Adv. Mater.*, 2010, **22**, 3361–3365.
8 D. Pires, J. L. Hedrick, A. De Silva, J. Frommer, B. Gotsmann, H. Wolf, M. Despont, U. Duerig and A. W. Knoll, *Science*, 2010, **328**, 732–735.
9 M. Rolandi, C. F. Quate and H. J. Dai, *Adv. Mater.*, 2002, **14**, 191–194.
10 P. Avouris, T. Hertel and R. Martel, *Appl. Phys. Lett.*, 1997, **71**, 285–287.
11 C. Cen, S. Thiel, J. Mannhart and J. Levy, *Science*, 2009, **323**, 1026–1030.
12 R. Maoz, E. Frydman, S. R. Cohen and J. Sagiv, *Adv. Mater.*, 2000, **12**, 725–728.
13 D. A. Unruh, C. Mauldin, S. J. Pastine, M. Rolandi and J. M. J. Frechet, *J. Am. Chem. Soc.*, 2010, **132**, 6890–6891.
14 H. J. Kreuzer, *Surf. Interface Anal.*, 2004, **36**, 372–379.
15 Z. M. Fresco, I. Suez, S. A. Backer and J. M. J. Frechet, *J. Am. Chem. Soc.*, 2004, **126**, 8374–8375.
16 Z. M. Fresco and J. M. J. Frechet, *J. Am. Chem. Soc.*, 2005, **127**, 8302–8303.
17 S. A. Backer, I. Suez, Z. M. Fresco, M. Rolandi and J. M. J. Frechet, *Langmuir*, 2007, **23**, 2297–2299.
18 X. N. Xie, M. Deng, H. Xu, S. W. Yang, D. C. Qi, X. Y. Gao, H. J. Chung, C. H. Sow, V. B. Tan and A. T. Wee, *J. Am. Chem. Soc.*, 2006, **128**, 2738–2744.
19 J. Germain, M. Rolandi, S. A. Backer and J. M. J. Frechet, *Adv. Mater.*, 2008, **20**, 4526–4529.
20 I. Suez, S. A. Backer and J. M. J. Frechet, *Nano Lett.*, 2005, **5**, 321–324.
21 I. Suez, M. Rolandi, S. A. Backer, A. Scholl, A. Doran, D. Okawa, A. Zettl and J. M. J. Frechet, *Adv. Mater.*, 2007, **19**, 3570–3573.
22 R. V. Martinez, N. S. Losilla, J. Martinez, Y. Huttel and R. Garcia, *Nano Lett.*, 2007, **7**, 1846–1850.
23 M. Rolandi, I. Suez, A. Scholl and J. M. J. Frechet, *Angew. Chem., Int. Ed.*, 2007, **46**, 7477–7480.
24 R. Garcia, N. S. Losilla, J. Martinez, R. V. Martinez, F. J. Palomares, Y. Huttel, M. Calvaresi and F. Zerbetto, *Appl. Phys. Lett.*, 2010, **96**, 143110.
25 J. D. Torrey, S. E. Vasko, A. Kapetanovic, Z. Zhu, A. Scholl and M. Rolandi, *Adv. Mater.*, 2010, **22**, 4639–4642.
26 H. Rauscher, F. Behrendt and R. J. Behm, *J. Vac. Sci. Technol., B*, 1997, **15**, 1373–1377.
27 A. M. Chockla and B. A. Korgel, *J. Mater. Chem.*, 2009, **19**, 996–1001.
28 K. R. Virwani, A. P. Malshe and K. P. Rajurkar, *Phys. Rev. Lett.*, 2007, **99**, 017601.
29 R. V. Martinez and R. Garcia, *Nano Lett.*, 2005, **5**, 1161–1164.